a factor of 5 at lower altitudes (~180 km), but charge exchange becomes dominant above about 210 km. The calculated C^+ values (Fig. 3) are significantly lower than the measured ones. The major loss process is $C^+ + CO_2 \rightarrow CO^+ + CO$ at the altitudes under consideration; therefore, the calculated C^+ densities depend on the assumed CO_2 values. The uncertainties in these CO_2 densities are, however, small compared to the discrepancy in C^+. These calculations appear to indicate that an important source mechanism has been ignored; one such possibility is charge exchange with neutral carbon.

The calculated N^+ densities are also too small; in calculating these densities the main source mechanism was dissociative photoionization of N_2 with the He^+ charge exchange also making some contributions. The major loss processes were charge exchange with CO_2 and CO. Atomic nitrogen is probably also present in the upper atmosphere of Venus (*14*), so that direct photoionization will have to be considered when some quantitative information on the abundance of N becomes available.

We assumed an NO density of 3×10^6 cm^{-3} at 150 km in order to get general agreement between the calculated and measured NO^+ densities in the region under consideration. The resulting major source and loss mechanisms are charge exchange of NO with O_2^+ and dissociative recombination, respectively. There is only indirect information available (*14*) on the neutral NO and N densities to provide some limits on these assumptions, and atomic nitrogen could have also been used to arrive at the measured NO^+ densities.

Both ion mass spectrometers (*11*) observed significant signals at mass 28, which is probably the result of the presence of both N_2^+ and CO^+ ions; CO^+ and N_2^+ are created mainly by dissociative and direct photoionization, respectively; charge exchange processes also make some contributions. The calculated CO^+ densities are larger by nearly an order of magnitude than the N_2^+ values. The sum of these CO^+ and N_2^+ densities (Fig. 3) does fall short of the measured values. However, if the measured C^+ densities are used in the calculations, a good agreement is obtained because of the rapid reaction $C^+ + CO_2 \rightarrow CO^+ + CO$. This indicates that the difficulty in the model traces back to problems in accounting for the C^+ values.

The calculations presented here are just the beginning of the analysis and interpretation of this great wealth of Pioneer Venus data. The comparisons of the measured and calculated ion density profiles have led to the following conclusions. (i) There is a reasonably good agreement between the calculated and measured gross behavior of the major ions except H^+, which may be influenced significantly by convective transport processes even during quiet conditions. (ii) Our present understanding of minor ion chemistry is incomplete at this time. (iii) The O/CO_2 ratio and the abundances of the minor neutral constituents (for example, N, NO, and C) play a very important role in determining the ion chemistry. (iv) The inhibition of diffusion by quasi-horizontal magnetic fields may be important. (v) Contributions to the daytime ion production rates by particle impact may also have to be considered if the peak density measured by the bus needs to be explained. Finally, we would emphasize that the data used in this report were restricted to relatively quiet conditions; composition and structure change significantly during disturbed conditions when convective flows and other solar wind-ionosphere interaction processes take over from the diffusive one at higher altitudes.

A. F. Nagy, T. E. Cravens
R. H. Chen
Space Physics Research Laboratory,
Department of Atmospheric and
Oceanic Science, University of
Michigan, Ann Arbor 48109
H. A. Taylor, Jr., L. H. Brace
H. C. Brinton
NASA Goddard Space Flight Center,
Greenbelt, Maryland 20771

References and Notes

1. A set of reports on the first results from the Pioneer Venus instruments was published in the 23 February 1979 issue of *Science*. Twelve of those papers dealt with the ionosheath-ionosphere-atmosphere of Venus, but for the sake of brevity they will not be referenced here individually.
2. R. H. Chen, thesis, University of Michigan (1977); ——— and A. F. Nagy, *J. Geophys. Res.* **83**, 1133 (1978); T. E. Cravens, A. F. Nagy, R. H. Chen, A. I. Stewart, *Geophys. Res. Lett.* **5**, 613 (1978).
3. L. H. Brace, R. F. Theis, J. P. Krehbiel, A. F. Nagy, T. M. Donahue, M. B. McElroy, A. Pedersen, *Science* **203**, 763 (1979); W. C. Knudsen, K. Spenner, R. C. Whitten, J. R. Spreiter, K. L. Miller, V. Novak, *ibid.*, p. 757.
4. T. E. Cravens, A. F. Nagy, L. H. Brace, R. H. Chen, W. C. Knudsen, *Geophys. Res. Lett.*, **6**, 341 (1979).
5. R. H. Chen, T. E. Cravens, A. F. Nagy, *J. Geophys. Res.* **83**, 3871 (1978).
6. H. E. Hinteregger, D. E. Bedo, J. W. Munson, D. B. Stillman, *Space Res.* **17**, 533 (1976), which was modified according to H. E. Hinteregger (personal communication).
7. P. M. Banks and G. Kockarts, *Aeronomy* (Academic Press, New York, 1973).
8. T. E. Cravens and A. E. S. Green, *Icarus* **33**, 612 (1978).
9. J. P. St. Maurice and R. W. Schunk, *Planet. Space Sci.* **25**, 907 (1976).
10. C. T. Russell, R. C. Elphic, J. A. Slavin, *Science* **203**, 745 (1979).
11. H. A. Taylor, Jr., *et al.*, *ibid.*, p. 752; H. A. Taylor, Jr., *et al.*, *ibid.*, p. 755.
12. R. E. Daniell, Jr., and P. A. Cloutier, *Planet. Space Sci.* **25**, 621 (1977).
13. A good compilation of the various rate coefficients used in this work may be found in D. L. Albritton, *At. Data Nucl. Data Tables* **22**, 1 (1978); for a subset of these reactions, together with a good discussion, see S. J. Bauer, T. M. Donahue, R. E. Hartle, H. A. Taylor, Jr., *Science* **205**, 109 (1979).
14. P. D. Feldman, H. W. Moos, J. T. Clarke, A. L. Lane, *Nature (London)* **279**, 221 (1979); A. I. Stewart and C. A. Barth, *Science* **205**, 59 (1979); D. W. Rusch and T. E. Cravens, in preparation.
15. We thank Drs. S. J. Bauer, T. Gombosi, D. M. Hunten, H. G. Mayr, and D. W. Rusch for numerous helpful discussions. Acknowledgment is also made to the National Center for Atmospheric Research sponsored by the National Science Foundation, for computing time used in this research. The work reported here was supported by NASA contracts NAS2-9130 and NGR23-005-015.

15 May 1979

Venus Ionosphere: Photochemical and Thermal Diffusion Control of Ion Composition

Abstract. *The major photochemical sources and sinks for ten of the ions measured by the ion mass spectrometer on the Pioneer Venus bus and orbiter spacecraft that are consistent with the neutral gas composition measured on the same spacecraft have been identified. The neutral gas temperature* (T_n) *as a function of solar zenith angle* (χ) *derived from measured ion distributions in photochemical equilibrium is given by* $T_n (K) = 323 \cos^{1/5}\chi$. *Above 200 kilometers, the altitude behavior of ions is generally controlled by plasma diffusion, with important modifications for minor ions due to thermal diffusion resulting from the observed gradients of plasma temperatures. The dayside equilibrium distributions of ions are sometimes perturbed by plasma convection, while lateral transport of ions from the dayside seems to be a major source of the nightside ionosphere.*

The first in situ ion composition measurements by the Bennett radio-frequency (RF) ion mass spectrometers on the Pioneer Venus bus and orbiter spacecraft revealed a complex ionosphere not fully anticipated by earlier theoretical models (*1*). The observed ion composition, however, is consistent with the neutral gas composition of the upper atmosphere measured by several Pioneer Venus instruments (*2*). In addition, direct measurements of the plasma temperatures (*3*) have important implications for the distribution of ions at altitudes where plasma diffusion becomes effective.

0036-8075/79/0706-0109$00.50/0

Table 1. Sources and sinks of ions in the Venus ionosphere (*5*).

Ion	Production rate (q)	Rate constant (J, sec^{-1}) (k, $\mathrm{cm}^3\ \mathrm{sec}^{-1}$)	Loss rate (L)	Rate constant (k, $\mathrm{cm}^3\ \mathrm{sec}^{-1}$) ($\alpha$, $\mathrm{cm}^3\ \mathrm{sec}^{-1}$)
1. H^+	$k_{11}[O^+][H]$	7(−10)*	$k_{12}[O][H^+]$	4(−10)
2. He^+	$J_2\,[He]$	1(−7)	$k_{22}[CO_2][He^+]$	1(−9)
3. O^{2+}	$J_3\,[O]$	2(−9)	$k_{23}[N_2][O^{2+}]$	2(−9)
4. C^+	$k_{41}[He^+][CO]$†	2(−9)	$k_{42}[CO_2][C^+]$	1(−9)
	$J_4\,[CO_2]$†	5(−8)		
5. N^+	$J_5\,[N_2]$†	8(−8)	$k_{52}[CO_2][N^+]$	1(−9)
6. O^+	$J_6\,[O]$	5(−7)	$k_{62}[CO_2][O^+]$	1(−9)
7. CO^+	$k_{71}[C^+][CO_2]$	2(−9)	$\alpha_7\,[O_2{}^+][CO^+]$	7(−7)
	$J_7\,[CO]$	9(−7)		
8. NO^+	$k_{81}[O^+][N_2]$†	1(−12)	$\alpha_8\,[O_2{}^+][NO^+]$	4(−7)
	$k_{82}[N^+][CO_2]$†	2(−11)		
9. $O_2{}^+$	$k_{91}[CO_2{}^+][O]$	1(−10)	$\alpha_9\,[O_2{}^+]^2$	2(−7)
	$k_{92}[O^+][CO_2]$	1(−9)		
10. $CO_2{}^+$	$J_{10}[CO_2]$	1(−6)	$k_{10}[O][CO_2{}^+]$	1(−10)
			$\alpha_{10}[O_2{}^+][CO_2{}^+]$	4(−7)

*$7 \times 10^{-10} \equiv 7(-10)$. †These production rates seem to be inadequate to account for the observed ion concentrations.

An evaluation of the appropriate time constants (*4*) shows that chemical processes should be important at altitudes below about 180 to 200 km, whereas above this altitude range, plasma diffusion should predominate. Using available information on neutral composition, electron temperatures, and ion temperatures (*2, 3*), we have assessed the role of physical and chemical processes controlling the ion composition to provide a guide for more detailed modeling investigations. A typical dayside ion composition of the Venus ionosphere (orbit 12) is shown in Fig. 1. Based on our evaluation of ion and neutral composition data (*1, 3*), the suggested principal sources and sinks of the ten ions illustrated in Fig. 1 are summarized in Table 1 (*5*). In addition to the ions listed here, the $^{18}O^+$ (18 amu) isotope of O^+ has been identified; mass 17 (identifiable as OH^+) has also been detected, but a large fraction is most likely the result of spillover from the O^+ mass peak. Consequently, it will probably be impossible to infer, from photochemical considerations, the presence and abundance of H_2.

As in the terrestrial ionosphere, H^+ is produced and lost by the resonant charge transfer reaction with O. The observed H^+ concentrations are consistent with the observed O^+, O, and H concentrations.

The O^{2+} ion appears to be the result of direct generation from O; production of O^{2+} by photoionization of O^+ does not seem to be consistent with the observed O^{2+} concentration in view of the recently measured large rate constant for its loss via N_2 (*6*). The altitude distribution of O^{2+} in chemical equilibrium favors loss of O^{2+} via N_2 rather than O, in contrast to the situation at Earth.

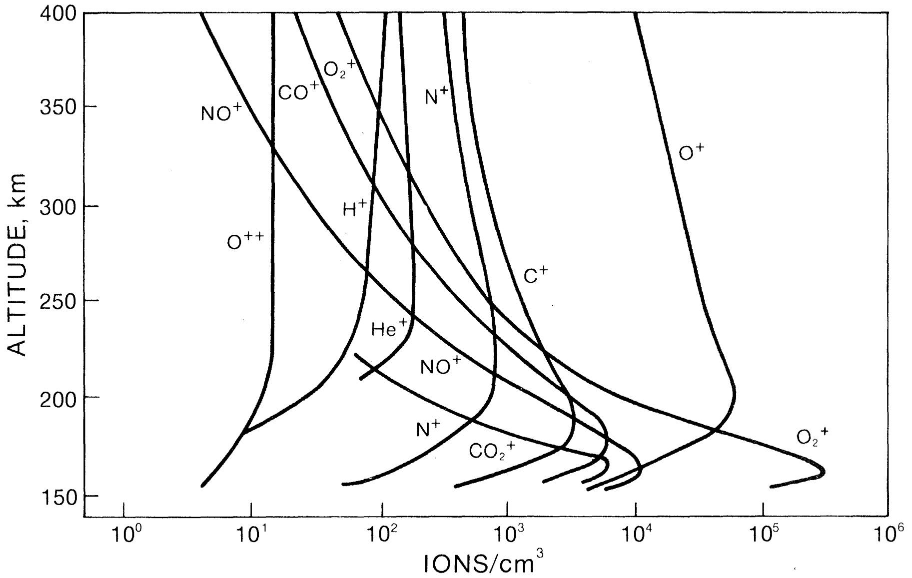

Fig. 1. Ion composition of the dayside ionosphere of Venus measured on orbit 12.

There is still a problem in accounting for the large abundance of the ion of mass 12, presumably C^+. Although the reaction between He^+ and CO seems to be a principal source of C^+ (*1*)—direct photoionization of C not being a possible source because of the lack of observed neutral C—the predominant loss process, the reaction with CO_2, requires a CO/CO_2 ratio larger than that indicated from the neutral mass spectrometer measurements. Further instrumental corrections, however, would tend to increase rather than decrease the CO/CO_2 ratio. An additional source of C^+ may be the dissociative ionization of CO_2, particularly at lower altitudes. The N^+ ion can best be accounted for by dissociative photoionization of N_2, an important constituent of the Venus upper atmosphere, and its loss via CO_2.

The concentration of the major atomic ion, O^+, is consistent with the observed O/CO_2 ratio derived from the neutral mass spectrometer measurements. Its predominance is directly associated with the fact that O becomes the predominant neutral constituent above ~ 150 km. Although the ion observed at mass 28 can be either $N_2{}^+$ or CO^+, photochemical considerations favor its identification as mainly CO^+. In view of the relatively large concentration of C^+, its reaction with CO_2, rather than photoionization of CO, seems to be the principal source of CO^+, while its loss is controlled by dissociative recombination. Unless neutral NO is present, NO^+ must be principally formed by charge transfer reactions between O^+ and N_2 and between N^+ and CO_2, and lost by dissociative recombination. The principal molecular ion, $O_2{}^+$, arises, as suggested before, from charge transfer between $CO_2{}^+$ and O and between O^+ and CO_2, and is lost by dissociative recombination. The $CO_2{}^+$ ion is produced by photoionization of CO_2 and lost by dissociative recombination and by charge transfer with O. Although the sources and sinks outlined above represent the most important and obvious ones in light of the presently known central composition and rate coefficients, more detailed model calculations seem to indicate that for some ions the sources considered here may still fall short (at least at the lower altitudes) of accounting for the observed ion concentrations (*7*).

From the condition $q = L$, the altitude distribution of the ions in chemical equilibrium can be determined. This altitude distribution usually appears in the form of products and ratios of constituents in-

Table 2. Thermal diffusion coefficients after Schunk and Walker (*10*).

Ion	α_j
H^+	−1.2
He^+	−1.1
O^{2+}	−0.4
C^+	−0.3
N^+	−0.1
O^+	0
CO^+	0.8
NO^+	0.9
O_2^+	1.0
CO_2^+	1.3

volved in the production and loss of a particular ion. In general, a scale height with an effective mass resulting from the involvement of the various neutral constituents can be defined, and for that reason ion distributions in chemical equilibrium can be used to determine the *neutral* gas temperature. This has been done, using several of the observed species for dayside orbits; the result is shown in Fig. 2.

The analytical fit of the experimental data implies that the neutral gas temperature at the subsolar point is $T_n = 323 \pm 30$ K. A test of this estimate for low solar zenith angles χ should become possible in early June 1979, when the periapsis of the orbit will cross the noon meridian. The neutral gas temperature derived from photochemical relations is in good agreement with that derived from the scale height of neutral constituents measured by the neutral mass spectrometers and the ultraviolet spectrometer. Because of the absence of photochemical equilibrium on the nightside, neutral gas temperatures cannot be derived with confidence from ion compositions for $\chi > 90°$. The temperature at the terminator, however, appears to be already representative of the nightside neutral gas temperatures, which range from 100 to 140 K (*8*).

Above about 180 km, the time constant for plasma diffusion becomes comparable to or shorter than the chemical lifetime, and the ion density distributions are therefore ideally expected to follow a diffusive equilibrium distribution. At about 200 km, O^+ reaches a maximum due to its increase with altitude under photochemical control and to the polarization field controlling its diffusion in the O_2^+ layer. Above this altitude, O^+ is the predominant ion and appears to be generally well represented by a diffusive equilibrium distribution. In contrast to the chemical equilibrium distributions, which reflect T_n, the diffusive equilibrium distributions reflect the electron and ion temperatures and their gradients. The gradients are of particular importance in the Venus ionosphere (*1*).

Because of the existence of plasma temperature gradients (∇T_p), thermal diffusion of ions, particularly of minor ones, should become important (*9, 10*). The altitude distribution of an ion X_j^+ (in terms of an altitude parameter z) under the control of diffusive processes, including thermal diffusion, can be approximated by (*4*)

$$\frac{1}{[X_j^+]}\frac{\partial [X_j^+]}{\partial z} = -\left[\left(m_j - \frac{Z_j m_+ T_e}{T_e + T_i}\right)\frac{g}{kT_i} + \frac{\partial (T_e + T_i)/\partial z}{T_e + T_i} - \frac{\alpha_j}{T_i}\frac{\partial T_i}{\partial z}\right] = -\frac{1}{H_j} \qquad (1)$$

where m_j and Z_j are the mass and charge of the particular ion, m_+ is the mean ion mass (that is, the mass of the predominant ion), g is the acceleration due to gravity and k is the Boltzmann constant, T_e and T_i are the electron and ion temperatures, respectively, and α_j is the thermal diffusion coefficient depending on the mass and charge ratios of the minor ion to the predominant ion. Numerical values for α_j for the ions under consideration are listed in Table 2. The effective scale height of the ion governed by the diffusive processes is H_j. For the predominant ion, this scale height can be expressed by

$$H = \frac{k(T_e + T_i)}{m_+ g + k\nabla(T_e + T_i)} \qquad (2)$$

Observed O^+ scale heights are generally in excellent agreement with the measured electron and ion temperatures and their gradients.

To assess the importance of thermal diffusion in the Venus ionosphere, Eq. 1 was evaluated for the ions under consideration, assuming $T_e = 2T_i$ and $\nabla T_e \simeq \nabla T_i = \nabla T_p \simeq 5$ K/km. The results of this analysis, expressed in terms of the ratios of the scale heights of particular ions to that of the predominant ion O^+ (which is not subject to thermal diffusion), are shown in Table 3. The important role of thermal diffusion in determining the scale heights of minor ions is apparent. Particularly sensitive indicators of thermal diffusion effects are He^+ and O^{2+}. Without thermal diffusion their densities would increase with altitude, while with thermal diffusion their densities would either decrease or be constant with altitude. Thermal diffusion causes the scale heights of the heavier minor ions to increase relative to values otherwise predicted whether there is a plasma temperature gradient or not.

Table 3. Scale height ratios for ions under diffusion control.

$\frac{H(X^+)}{H(O^+)}$	$\nabla T_p = 0$ $T_e = 2T_i$	∇T_p (no thermal diffusion)	∇T_p (thermal diffusion)	Observed ratio
H^+	−0.6*	−1.4	−15.3	~−10
He^+	−0.8	−2.6	4	~3
O^{2+}	−16	−4.3	∞	∞
C^+	4	1.9	1.4	~1
N^+	1.6	1.3	1.2	~1
CO^+	0.31	0.42	0.51	
NO^+	0.28	0.38	0.48	~0.5
O_2^+	0.25	0.35	0.45	
CO_2^+	0.16	0.26	0.30	~0.3

*A negative value implies that $H_j < 0$; that is, $\partial \ln [X_j^+]/\partial z > 0$.

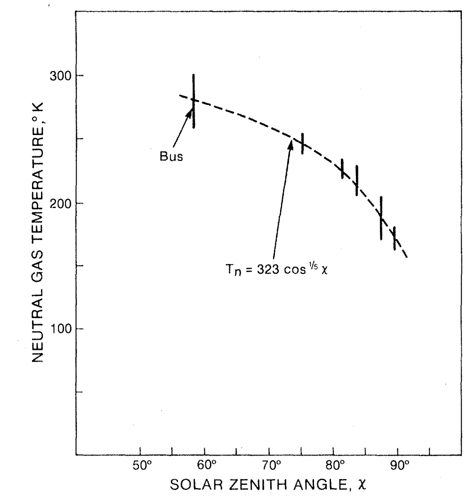

Fig. 2. Neutral gas temperature as function of solar zenith angle, derived from ion density distributions measured by the ion mass spectrometers on the bus and orbiter spacecraft by using photochemical relations. The temperatures are representative of the altitude range $160 \lesssim h \lesssim 180$ km; that is, near the exobase. For $\chi \gtrsim 85°$, cos χ is determined by the Chapman function (*4*).

Although the dayside ionosphere of Venus appears to be under diffusive control for relatively quiet conditions, there are cases in which diffusive equilibrium distributions of ions are modified by convective plasma transport processes (*11*). For the nightside ionosphere, however, simple chemical and diffusive equilibrium distributions most often seem to be inadequate to describe the observations because of the strong role of lateral plasma transport of ions from the dayside (*12*).

SIEGFRIED J. BAUER
NASA/Goddard Space Flight Center, Greenbelt, Maryland 20771
THOMAS M. DONAHUE
University of Michigan, Ann Arbor
RICHARD E. HARTLE
HARRY A. TAYLOR, JR.
NASA/Goddard Space Flight Center

References and Notes

1. H. A. Taylor, Jr., *et al.*, *Science* **203**, 752 (1979).
2. H. B. Niemann, R. E. Hartle, W. T. Kasprzak, N. W. Spencer, D. M. Hunten, G. R. Carignan, *ibid.*, p. 770; U. von Zahn, D. Krankowsky, K. Mauersberger, A. O. Nier, D. M. Hunten, *ibid.*, p. 768; A. I. Stewart, D. E. Anderson, Jr., L. W. Esposito, C. A. Barth, *ibid.*, p. 777.
3. W. C. Knudsen, K. Spenner, R. C. Whitten, J. R. Spreiter, K. L. Miller, V. Novak, *ibid.*, p. 757; L. H. Brace *et al.*, *ibid.*, p. 763.
4. S. J. Bauer, *Physics of Planetary Ionospheres* (Springer-Verlag, New York, 1973).
5. The reaction rates are taken from standard reference works, such as those by P. M. Banks and G. Kockarts [*Aeronomy* (Academic Press, New York, 1973), parts A and B]; S. J. Bauer (*4*); and D. G. Torr and M. R. Torr [*Rev. Geophys. Space Phys.* **16**, 327 (1978)]. Most of the photoionization rate constants (*J*) are adaptations for Venus from a recent evaluation for the terrestrial thermosphere by K. Kirby, E. R. Constantinides, S. Babeu, M. Oppenheimer, and G. A. Victor (*At. Data*, in press).
6. Double photoionization of O has been proposed by G. A. Victor and E. R. Constantinides (in preparation). The new loss rate for O^{2+} has been measured by R. Johnson and M. Biondi [*Geophys. Res. Lett.* **5**, 847 (1978)] and F. A. Howorka, A. Viggiano, D. L. Albritton, E. E. Ferguson, and F. C. Fehsenfeld (in preparation).
7. A. F. Nagy, T. E. Cravens, R. H. Chen, H. A. Taylor, Jr., L. H. Brace, H. C. Brinton, *Science* **205**, 107 (1979).
8. H. B. Niemann, R. E. Hartle, A. E. Hedin, W. T. Kasprzak, N. W. Spencer, D. M. Hunten, G. R. Carignan, *ibid.*, p. 54; A. I. Stewart and C. A. Barth, *ibid.*, p. 59.
9. S. Chapman, *Proc. Phys. Soc. London* **72**, 335 (1958); J. C. G. Walker *Planet. Space Sci.* **15**, 1151 (1967).
10. R. Schunk and J. C. G. Walker, *Planet. Space Sci.* **17**, 853 (1969).
11. H. A. Taylor, Jr., *et al.*, *Science* **203**, 755 (1979).
12. H. A. Taylor, Jr., H. C. Brinton, S. J. Bauer, R. E. Hartle, P. A. Cloutier, R. E. Daniell, Jr., T. M. Donahue, *ibid.* **205**, 96 (1979).

15 May 1979

Absorption of Whistler Mode Waves in the Ionosphere of Venus

Abstract. *It is shown that whistler mode waves from the ionosheath of Venus are absorbed by Landau damping at the dayside ionosphere boundary. This process heats the ionospheric electrons and it may provide an important energy input into the dayside ionosphere. Cyclotron damping of the waves does not occur in the same region. However, Landau damping of ionosheath waves is apparently not an important energy source in the nightside ionosphere. Impulsive events in the nightside ionosphere seem to fall into two classes: (i) lightning signals (near periapsis) and (ii) noise, which may be caused by gradient or current instabilities.*

The Pioneer Venus mission was designed to provide definitive answers to a number of important questions about Venus, including those having to do with the mechanism of energy transfer from the solar wind to the ionosphere and upper atmosphere. In reviewing plans for the mission it was noted that the studies of simple static pressure balance would have to be combined with an analysis of dynamical dissipation processes at the ionosphere boundary (*1*), and several of the initial reports on data from the Pioneer Venus orbiter made reference to this problem. It was shown that the dayside ionopause is characterized by an approximate pressure balance relationship (*2–4*), and it was also shown that during quiet times, the density and temperature profiles in the upper ionosphere are consistent with a topside energy deposition on the order of (3 to 7) × 10^{-2} erg/cm^2-sec (*3, 4*). The initial analysis of the wave observations suggested that damping of 100-Hz waves (assumed to be whistler mode turbulence) at the ionopause could provide an average of 5 × 10^{-2} erg/cm^2-sec as a local energy source of ionospheric and atmospheric processes (*5*).

In this report we examine critically the concept of damping of whistler mode waves by ionospheric electrons. We use simultaneous, high-time-resolution orbiter measurements of the electron density and temperature, the magnetic field magnitude, and the 100-Hz wave amplitude, and we demonstrate that the Landau damping picture has quantitative validity at the dayside ionopause. We also discuss briefly cyclotron damping and the nightside low-altitude observations, which are characterized by the detection of undamped whistler mode signals apparently associated with atmospheric lightning.

The initial discussion of wave damping by ionospheric electrons was based on data averaged over a number of spin periods from orbit 4 (*5*). We have selected orbit 3 in order to present the quantitative analysis, and Fig. 1 shows details. Figure 1a contains averages (over one spin period) of the 100-Hz power levels (more precisely, values of the electric field spectral density) from the electric field detector. The electron temperature and density data were averaged over a single spin period, as were the magnetic field data. The outbound ionopause was crossed between 1437 and 1438 (spacecraft event time), and we explore here the associated change of the spectral density in terms of wave damping and energy transfer to the ionospheric electrons.

At the start, it is necessary to consider again the previous tentative identification of these 100-Hz waves as whistler mode oscillations. The orbiter wave investigation has limited frequency coverage; it measures only electric fields; and the sun-oriented sheath modulation makes it difficult to carry out a precise polarization analysis. Nevertheless, we have analyzed the wave polarization with respect to the magnetic field direction in the ionosheath (after 1448, for instance), and we find no evidence that these waves have polarization characteristic of electrostatic waves. Some additional guidance comes from a comparison of observations in Earth's magnetosheath with these Venus ionosheath observations. For example, at Earth, simultaneous high-time-resolution electric and magnetic field measurements from the International Sun-Earth Explorer ISEE 1 show that for frequencies $f \leq 56$ Hz the dominant magnetosheath waves have essentially identical amplitude variations (*6*). Thus these magnetosheath waves with $f << f_c$, the electron cyclotron frequency, are certainly electromagnetic whistler mode waves, although the higher frequency turbulence in the same region (including some waves with $f < f_c$) is likely to be electrostatic (*7*). However, since the interplanetary magnetic field at Venus is nominally about 1.8 times as high as that value at 1 AU, the corresponding wave and cyclotron frequencies must be scaled upward by that factor. This scaling suggests that in the Venus ionosheath the 100-Hz channel corresponds to the 56-Hz channel in Earth's magnetosheath, and this extrapolation then indicates that the whistler mode identification is correct for our 100-Hz measurements.

For plasma waves such as obliquely propagating whistlers, strong wave-particle interactions occur when a significant number of the charged particles in the plasma move with velocities close to the phase velocity of the wave. For a plasma with a thermal (Maxwellian) distribution of particles, strong damping occurs when the wave phase speed is equal to the thermal speed (most probable speed), and this is called Landau damping. This matching of speeds means that in its rest frame the "average" charged particle is acted on by a d-c electric field, and the particle is accelerated, gaining energy at the expense of the wave energy. A related type of resonant damping occurs when waves appear Doppler shifted to the gyrofrequency of the particles. This damping is called cyclotron damping. The energy of the resonant particles parallel to the wave velocity may be computed from the phase velocity. For whistler mode waves and electrons, the Landau resonant energy is

$$E_L \simeq \frac{B^2}{8\pi N_e \cos\theta}\left(\frac{f}{f_c}\right) \qquad (1)$$